ISSN 0036-0244, Russian Journal of Physical Chemistry A, 2016, Vol. 90, No. 1, pp. 1–10. © Pleiades Publishing, Ltd., 2016.
Original Russian Text © M.A. Shevchenko, M.I. Ivanov, V.V. Berezutski, V.S. Sudavtsova, 2016, published in Zhurnal Fizicheskoi Khimii, 2016, Vol. 90, No. 1, pp. 3–12.

CHEMICAL THERMODYNAMICS AND THERMOCHEMISTRY

Thermodynamic Properties of Alloys of the Binary Gd–In System[1]

M. A. Shevchenko, M. I. Ivanov, V. V. Berezutski, and V. S. Sudavtsova
Frantsevich Institute for Problems of Materials Science, ul. Krzhyzhanovskogo 3, Kyiv, 03142 Ukraine
e-mail: sud@ipms.kiev.ua, maximshevch@ukr.net

Received December 22, 2014

Abstract—The thermochemical properties of melts of the binary Gd–In system were studied by the calorimetry method at 1470–1700 K over the whole concentration interval. It was shown that significant negative heat effects of mixing are characteristic features for these melts. Using the ideal associated solution (IAS) model, the activities of components, Gibbs energies and the entropies of mixing in the alloys of this systems and its phase diagram were calculated. They agree with the data from literature.

Keywords: calorimetry, melts, thermodynamic properties, enthalpies, activities, gadolinium, indium.

DOI: 10.1134/S0036024415120274

Alloys of rare–earth metals with p–elements of the third group are promising as superconductors, catalysts and promoters, as well as materials for cathodes with various emission properties [1, 2]. However, there are only few works in literature devoted to investigation of thermodynamic properties of indium with lanthanides. Those investigations were mostly conducted with alloys containing 75% or more indium. This can be explained by limited availability of the components in pure state, combined with instability of their alloys in air. A complete thermodynamic analysis made using CALPHAD method is known only for the systems In–La [2] and In–Eu(Yb) [3].

Nevertheless, other features make these alloys rather easy objects of investigations: that is, they are mostly low–melting, non–volatile, and do not react with the refractory metals used as crucible materials. This allows conducting the investigation of thermodynamic properties of the In–Ln melts using calorimetry method over wide concentration ranges, which has been done successfully by us for the Eu–In [4] and the Ce–In systems. The present work is dedicated to the melts of the Gd–In system. Furthermore, the upcoming data for the enthalpies of mixing of melts of the In–La and In–Yb systems will allow determining the regularities and tendencies of the interaction of components in the row of the In–Ln systems.

The phase diagram of the Gd–In system was studied in three works [5–7], the results of which are different. A discussion of these works was made by Palenzona [8], and the preference was given to the data [7]. The phase diagram contains four congruently melting intermetallics: Gd_2In, GdIn (more exact composition of which is $Gd_{10}In_9$), Gd_3In_5, and $GdIn_3$. The compound Gd_5In_3 melts incongruently, but in [7, 8] the liquidus slope of its equilibrium with the melt is very steep, that calls for doubtfulness of this part of the phase diagram. In addition, both modifications (α- and β-) Gd form solid solutions with significant fraction of indium (up to 10–15%). The solubility of Gd in liquid In (actually, the liquidus curve of equilibrium of the $GdIn_3$ compound with the melt) at 800–1000 K was described by equation $\log x_{\mathrm{Gd}} = -1.6 - 878/T$ in [9].

Investigations of thermodynamic properties of alloys of the Gd–In systems were limited by indium–rich ranges and relatively low temperatures. So, in the works [10–13] the melts with 0–25% Gd were studied by e.m.f. method at 638–1011 K. The enthalpy of formation of the $GdIn_3$ compound was determined by calorimetry method at: –45.7 ± 2.5 kJ/mol [14] and –48.5 ± 2.2 kJ/mol [15].

Thermodynamic properties of dilute solutions of Gd in liquid In are described in [16] by an equation $\log\gamma_{\mathrm{Gd}} = 2.876 - 10\,818/T$, whence $\Delta\overline{H}^{\infty}_{\mathrm{Gd}} =$ –207.1 kJ/mol, $\Delta\overline{S}^{\infty\mathrm{ex}}_{\mathrm{Gd}} = -55.1$ J/(mol K), $\Delta\overline{G}^{\infty\mathrm{ex}}_{\mathrm{Gd}} =$ –163.0, –157.5, and –152.0 kJ/mol at 800, 900, and 1000 K, respectively. Likewise, the reviews [17, 18] do not contain any self–consistent assessment of thermodynamic properties and phase equilibria in the Gd–In system. In the work [19], the thermodynamic properties of intermetallics $LnIn_3$ are described by general dependence from temperature and the atomic number of the lanthanide (excluding Eu, Yb). A decrease of exothermic values of the enthalpies of formation of $LnIn_3$ from –58...–55 kJ/mol for light lanthanides to –35 kJ/mol for Lu is observed. Accordingly to those dependences,

---

[1] The article was translated by the authors.

Table 1. Experimental values of the partial and integral enthalpies of mixing of the melts of the Gd–In system (kJ/mol)

Series 1			Series 2			Series 3		
x_{In}	$-\Delta\overline{H}_{\mathrm{In}}$	$-\Delta H$	x_{In}	$-\Delta\overline{H}_{\mathrm{In}}$	$-\Delta H$	x_{In}	$-\Delta\overline{H}_{\mathrm{Gd}}$	$-\Delta H$
1650 K			1670 K			1470 K		
0.0137	109.2	1.50	0.0200	112.7	2.25	0.9922	126.9	0.98
0.0270	110.0	2.96	0.0311	113.9	3.52	0.9843	126.9	1.99
0.0401	109.0	4.38	0.0431	107.9	4.81	0.9763	124.5	2.99
0.0531	108.0	5.79	0.0551	101.6	6.02	0.9684	133.1	4.04
0.0662	102.8	7.14	0.0669	106.6	7.28	0.9603	129.7	5.09
0.0793	113.0	8.62	0.0784	114.7	8.60	0.9521	123.9	6.11
0.0926	112.4	10.12	0.1020	111.7	11.24	0.9438	127.3	7.16
0.1058	114.5	11.63	0.1139	114.4	12.62	0.9356	130.6	8.23
0.1187	111.9	13.08	0.1221	112.2	13.53	1500 K		
0.1318	102.5	14.40	0.1453	109.4	16.06	0.9171	121.4	10.47
0.1408	102.1	15.32	0.1569	113.7	17.40	0.9106	117.6	11.23
0.1531	108.3	16.65	0.1686	107.4	18.64	0.9034	123.9	12.13
0.1657	110.8	18.05	0.1801	104.9	19.83	0.8945	113.7	13.13
0.1786	107.6	19.43	0.1902	99.4	20.81	0.8872	119.6	14
0.1913	108.9	20.82	0.2005	100.4	21.83	0.8791	123.1	14.99
0.2039	106.9	22.16	0.2105	89.8	22.68	0.8709	114.8	15.92
0.2163	88.4	23.19	0.2197	90.5	23.47	0.8628	116.0	16.85
0.2285	99.6	24.37	1620 K			0.8547	116.2	17.78
0.2402	97.9	25.49	0.2277	104.4	24.29	0.8469	118.9	18.70
0.2517	93.3	26.52	0.2367	96.6	25.14	0.8407	117.6	19.43
0.2629	89.4	27.46	0.2460	87.6	25.90	0.8342	121.1	20.22
1580 K			0.2553	90.7	26.70	0.8276	114.4	20.96
0.2662	88.3	27.73	0.2645	85.9	27.43	0.8268	122.5	21.07
0.2760	100.7	28.71	0.2735	97.1	28.28	0.8205	118.1	21.81
0.2862	86.9	29.53	0.2823	86.1	28.99	0.8141	119.0	22.56
0.2963	88.7	30.37	0.2911	81.1	29.62	0.8077	119.3	23.32
0.3063	79.9	31.07	0.2968	77.9	30.01	0.8012	113.2	24.04
0.3160	918	31.92	0.3050	92.4	30.74	1530 K		
0.3257	83.2	32.66	0.3132	82.2	31.34	0.7949	107.3	24.70
0.3352	73.9	33.23	0.3212	69.4	31.79	0.7887	103.8	25.32
			0.3447	70.8	33.10	1550 K		
			0.3522	68.6	33.51	0.7836	108.3	25.85
			0.3565	63.7	33.80	0.7785	112.4	26.41
			0.3635	77.0	34.27	0.7733	109.9	26.97
			0.3705	62.4	34.73	0.7672	111.4	27.63
			0.3773	80.0	35.22	1600 K		
			1670 K			0.7610	98.1	28.20
			0.3834	64.3	35.50	0.7547	96.5	28.77
			0.3894	62.6	35.77	0.7486	95.8	29.32
			0.3953	70.2	36.10	0.7425	93.2	29.84
			0.4012	68.9	36.42	0.7365	102.6	30.42

Table 1. (Contd.)

Series 1			Series 2			Series 3		
x_{In}	$-\Delta\overline{H}_{\text{In}}$	$-\Delta H$	x_{In}	$-\Delta\overline{H}_{\text{In}}$	$-\Delta H$	x_{In}	$-\Delta\overline{H}_{\text{Gd}}$	$-\Delta H$
			0.4070	62.8	36.68	0.7305	99.8	30.98
			0.4127	53.8	36.84	0.7247	97.0	31.51
			0.4185	59.1	37.06	0.7189	96.8	32.04
			0.4243	55.9	37.25	0.7131	95.5	32.54
			0.4302	58.9	37.47	0.7074	91.0	33.01
			0.4359	57.1	37.67	0.7018	94.6	33.50
				1700 K		0.6962	90.7	33.96
			0.4414	51.4	37.80	0.6906	81.3	34.34
			0.4469	52.7	37.95	0.6851	90.7	34.78
			0.4523	48.5	38.05	0.6797	89.4	35.22
			0.4577	53.0	38.20	0.6743	76.9	35.55
			0.4630	55.5	38.37	0.6690	85.3	35.94
			0.4682	54.8	38.53	0.6636	83.9	36.32
			0.4733	50.8	38.64	0.6584	84.9	36.71
			0.4806	52.3	38.83	0.6531	79.1	37.05
			0.4855	49.8	38.94	0.6479	73.2	37.34
			0.4903	50.0	39.04	0.6427	74.4	37.63
				1670 K		0.6374	77.4	37.96
			0.4940	49.4	39.12	0.6322	74.1	38.26
			0.4974	48.5	39.20		1620 K	
						0.6274	65.2	38.46
						0.6222	58.0	38.62
						0.6170	59.0	38.79
						0.6118	55.5	38.93
						0.6067	54.1	39.06
						0.6016	49.8	39.15
						0.5966	45.2	39.20
						0.5915	43.1	39.23
						0.5864	45.1	39.28
						0.5814	47.5	39.35
						0.5763	55.4	39.50

for GdIn_3 $\Delta_f H^{298} = -47.6$ kJ/mol, $\Delta_f H^{775} = -51.3$ kJ/mol, that correlates with the data [10–15].

So, the information about the thermochemical properties of melts over the whole concentration range of the Gd–In system, as well as of the gadolinium-rich intermetallics, is absent in literature; that is why their determination is of great interest. The goal of the present work is measurement of the enthalpies of mixing of melts of the Gd–In system using isoperibolic calorimetry, and creation of the thermodynamic model to describe all experimental data (our and taken from literature, including the phase diagram).

EXPERIMENTAL

A full description of our experimental technique was given in [20]. The experiments over the whole concentration range were conducted in molybdenum crucibles. Owing to maintenance of as low temperatures as possible to keep the Gd–In alloys liquid, we managed to avoid the loss of mass due to evaporation

Table 2. Partial and integral enthalpies of mixing of the Gd–In system at 1600 K, kJ/mol

x_{In}	$-\Delta H$	$-\Delta\overline{H}_{\text{Gd}}$	$-\Delta\overline{H}_{\text{In}}$
0	0	0	111.6 ± 7.0
0.1	11.0 ± 0.3	0.2 ± 0.0	107.7 ± 6.8
0.2	21.4 ± 0.6	1.7 ± 0.1	100.0 ± 6.3
0.3	30.3 ± 0.9	7.2 ± 0.4	84.4 ± 5.3
0.4	36.5 ± 1.1	18.6 ± 1.0	63.4 ± 4.0
0.5	39.4 ± 1.2	32.6 ± 1.7	46.2 ± 2.9
0.6	39.0 ± 1.2	54.1 ± 2.9	29.0 ± 1.8
0.7	33.9 ± 1.0	88.2 ± 4.7	10.7 ± 0.7
0.8	24.2 ± 0.7	112.1 ± 5.9	2.2 ± 0.1
0.9	12.4 ± 0.4	121.9 ± 6.5	0.3 ± 0.0
1	0	126.5 ± 6.7	0

of the components, and the interaction of melts with the crucible materials.

Two series of experiments were conducted from the Gd side, and one series from the In side (Table 1). At the beginning of the experiments, the mass of the metal in the crucible was 1.5–1.9 g; the masses of samples dropped into the crucible were 0.014–0.037 g. The calorimeter was calibrated at the beginning of each series with the same metal as placed in the crucible. Then, the difference between the enthalpies of the liquid metal at the temperature of the experiment, and of the solid metal at the room temperature (298 K) was calculated accordingly to [21]. During each series, the calibration was periodically repeated, alternating 3–4 calibration samples with 10–20 samples of the second component. For repeated calibrations, we used the same metal (first component), the partial enthalpies of which are small and available for calculation using the Gibbs–Duhem equation; otherwise, we used molybdenum samples. The repetitive calibrations allowed us to detect the change of the heat exchange coefficient of the calorimeter (i.e. its effective heat capacity), which gradually increased approximately 1.5 times during each series, due to the increase of the mass of the alloy in the crucible.

The partial mixing enthalpies of the components ($\Delta\overline{H}_i$) were calculated using the equation

$$\Delta\overline{H}_i = -\Delta H_{298}^{T_0}(i) + \frac{k}{n_i}\int_{\tau_0}^{\tau_\infty}(T - T_0)dt,$$

where k is the heat exchange coefficient of the calorimeter, determined from the calibration component A as:

$$k = \Delta H_{298}^{T_0}(A)\,n_A \Big/ \int_{\tau_0}^{\tau_\infty}(T - T_0)\,dt.$$

$\Delta H_{298}^{T_0}(i)$ is the enthalpy difference between the liquid metal i at the temperature of the experiment, and the solid metal at room temperature [21]; n_i is the molar quantity of the metal in the sample; $\int_{\tau_0}^{\tau_\infty}(T - T_0)dt$ is the area below the peak on the thermogram (τ_0, τ_∞ are times of the beginning and the end of the heat effect recording, T is temperature, T_0 is equilibrium temperature of the crucible, t is time).

The integral enthalpies of mixing of the melt were calculated using a recurrent equation

$$\Delta H^{n+1} = \Delta H^{n} + \left(\Delta\overline{H}_i^{\,n+1} - \Delta H^{n}\right)\left(x_i^{n+1} - x_i^{n}\right)\Big/\left(1 - x_i^{n}\right),$$

which is accurate in the case of small change of the concentration of the component i from x_i^n to x_i^{n+1} when the $(n+1)$th sample is added.

The experimental values of $\Delta\overline{H}_{\text{In,Gd}}$ and ΔH are given in the Table 1.

The obtained experimental points were described by smoothed concentration dependences accordingly to the model of ideal associated solutions (IAS, see below). The difference of temperatures ±100 K between various experiments was neglected. The partial and integral enthalpies of mixing of the Gd–In system at 1600 K are presented in the Fig. 1, an their smoothed values at rounded concentrations, with the errors, in the Table 2. The errors were evaluated from the mean square deviations of the experimental points from the smooth curves. For each of the functions ΔH, $\Delta\overline{H}_{\text{Gd}}$, $\Delta\overline{H}_{\text{In}}$, they were assumed proportional to absolute value of the function.

Since the calculation of thermodynamic properties using IAS model requires special software that is not always available, it is desirable to give an alternative simple expression of the concentration dependences of the thermodynamic properties. This expression describes the experimental data with worse precision, and does not account for the temperature dependence, thus it is valid only for $T = 1600 \pm 100$ K. Such polynomial expressions of the partial and integral enthalpies of mixing (kJ/mol) are given below:

$$\Delta\overline{H}_{\text{In}} = (1 - x_{\text{In}})^2 \times\left(-111.6 - 229.1x_{\text{In}} - 47.3x_{\text{In}}^2 + 461.9x_{\text{In}}^3\right);$$

$$\Delta\overline{H}_{\text{Gd}} = x_{\text{In}}^2\left(2.9 - 197.6x_{\text{In}} - 393.7x_{\text{In}}^2 + 461.9x_{\text{In}}^3\right);$$

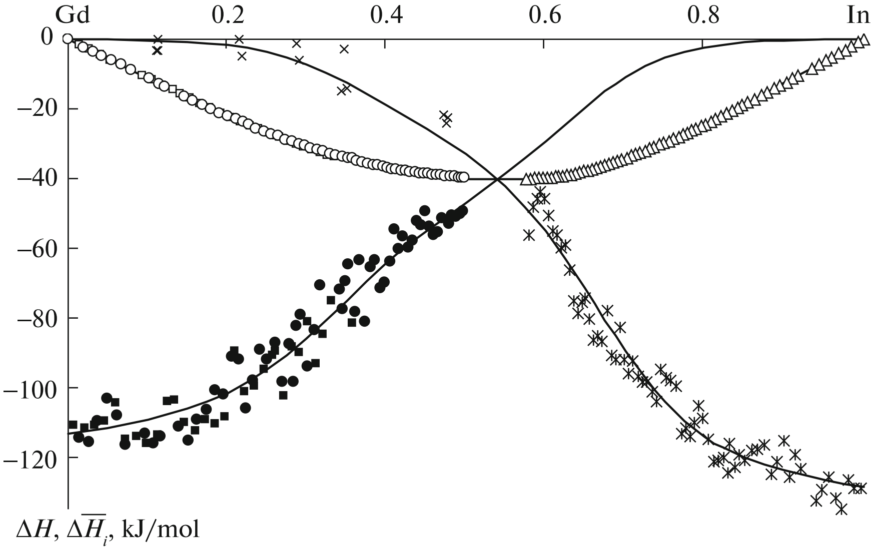

Fig. 1. Partial and integral mixing enthalpies of melts of the Gd–In system, studied by us experimentally (series 1: ■ $\Delta\overline{H}_{\mathrm{In}}$, □ ΔH; series 2: ● $\Delta\overline{H}_{\mathrm{In}}$, ○ ΔH, × $\Delta\overline{H}_{\mathrm{Gd}}$; series 3: ⚹ $\Delta\overline{H}_{\mathrm{Gd}}$, △ ΔH) and approximated using IAS model (——).

$$\Delta H = x_{\mathrm{In}}(1 - x_{\mathrm{In}}) \times \left(-111.6 - 114.5x_{\mathrm{In}} - 15.8x_{\mathrm{In}}^2 + 115.5x_{\mathrm{In}}^3\right).$$

The integral excess mixing entropies are approximated by the expression

$$\Delta S^{\mathrm{ex}} = x_{\mathrm{In}}(1 - x_{\mathrm{In}})\left(-34.4 - 45.6x_{\mathrm{In}} - 18.5x_{\mathrm{In}}^2 + 57{,}4x_{\mathrm{In}}^3\right), \ \mathrm{J/(mol\ K)}.$$

MODELING RESULTS AND DISCUSSION

The obtained data together with the data from literature were treated using the software package developed in our laboratory, based on the ideal associated solution model (IAS). We have used this methodology many times before, to treat the results of calorimetric investigation of various melts in complex with the data from literature on the phase equilibria and thermodynamic properties of those systems with strong interaction between the components [22–24]; the correctness of this methodology for such systems was proved in [25]. Apparently, this model is unsuitable only for description of the thermodynamic properties of melts of the metallic systems with positive mixing enthalpies.

All available experimental data, along with the list of the compounds in the solid alloys (accordingly to the phase diagram), and of the anticipated associates in the melts, were inserted into our program. Arbitrary starting values of the enthalpies ($\Delta_{\mathrm{f}}H^{\mathrm{sol}}$, $\Delta_{\mathrm{f}}H^{\mathrm{liq}}$) and entropies ($\Delta_{\mathrm{f}}S^{\mathrm{sol}}$, $\Delta_{\mathrm{f}}S^{\mathrm{liq}}$) of formation of these compounds in the solid alloys and associates in the liquid phase were set, and these values were variables during the optimization process. If the chosen set of associates is correct, and the data from literature are not controversial, it is possible to achieve satisfactory agreement with all that experimental data for the alloys at some values of the variable parameters.

The equilibrium concentrations (molar fractions) of the associates at given composition and temperature are evaluated by minimizing the function

$$\Delta G = RT\left(a_A \ln a_A + a_B \ln a_B + \sum_{n=1}^{N} x_n\left(\frac{\Delta G_n}{RT} + \ln x_n\right)\right)\Bigg/\left(1 + \sum_{n=1}^{N}(i_n + j_n - 1)x_n\right),$$

where $\Delta G_n = \Delta_{\mathrm{f}}H_n^{\mathrm{liq}} - T\Delta_{\mathrm{f}}S_n^{\mathrm{liq}}$; $a_A = x_{A_1}$ and $a_B = x_{B_1}$ are molar fractions of the monomers, which are equal to the activities of the components accordingly to the model principles; x_n are molar parts of the associates. The normalizing conditions are

$$a_A + a_B + \sum_{n=1}^{N} x_n = 1,$$

$$1 - x_A = x_B = \left(a_B + \sum_{n=1}^{N} x_n j_n\right)\Bigg/\left(a_A + a_B + \sum_{n=1}^{N} x_n(i_n + j_n)\right),$$

where x_A, x_B are the general molar fractions of the components in the melt.

When the minimum of ΔG and the corresponding values of a_A, a_B, and x_n $(n = 1\ldots N)$ are found, it is

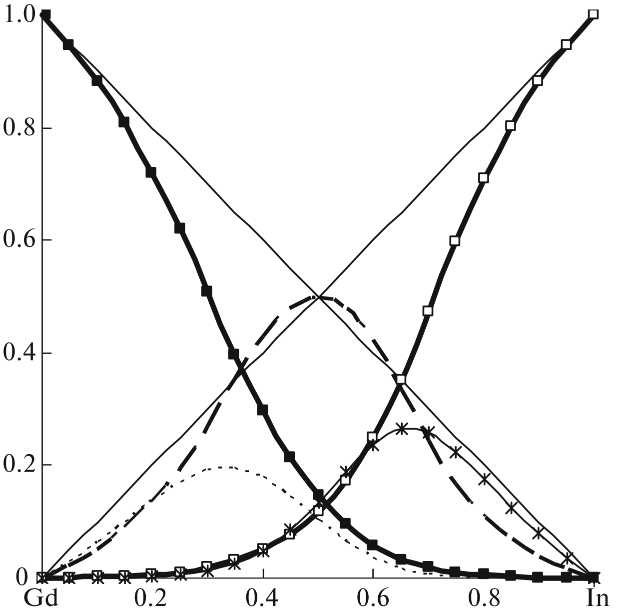

Fig. 2. Activities of the components (a_i: —■— Gd, —□— In) and molar fractions of the associates (x_i: ------ Gd_2In, — — GdIn, —✳— $GdIn_2$) in the melts of the Gd–In system at 1600 K, accordingly to IAS model.

possible to calculate other thermodynamic functions, e.g.,

$$\Delta H = \left(\sum_{n=1}^{N} \Delta_f H_n x_n\right) \Bigg/ \left(1 + \sum_{n=1}^{N} (i_n + j_n - 1) x_n\right).$$

We used self-made programs to compute the thermodynamic properties from the values of the parameters $\Delta_f H_n^{liq}$ and $\Delta_f S_n^{liq}$, and to optimize these parameters for closest identity of thermodynamic properties to the experimental data.

Table 3. Enthalpies (kJ/mol) and entropies (J/(mol K)) of formation of the associates (liq) and intermetallics (sol) in the Gd–In system at 298 K

Composition	$-\Delta_f H^{liq}$	$-\Delta_f S^{liq}$	$-\Delta_f H^{sol}$	$-\Delta_f S^{sol}$
Gd_2In	43.1	16.7	38.7	8.4
Gd_5In_3			42.7	10.0
$Gd_{10}In_9$			48.0	11.0
GdIn	45.3	14.4		
Gd_3In_5			50.3	13.2
$GdIn_2$	48.0	18.4		
$GdIn_3$			45.3	12.7

A three-associate model, considering formation of the associates Gd_2In, GdIn, and $GdIn_2$, appeared sufficient for satisfactory description of the thermodynamic properties of the Gd–In system. The two first of these associates have similar compositions to congruently-melting intermetallics of the Gd–In system; the composition of the third associate lies between the compounds Gd_3In_5 and $GdIn_3$. We tried to consider the existence of other, more complex associates, for example $GdIn_3$; but that did not improve the description of the experimental data.

The obtained parameters of the IAS model for the Gd–In system are listed in the Table 3.

Most solid phases were considered stoichiometric, and for only some of them a possibility of the homogeneity range was accounted by introducing the concentration dependences of the Gibbs energy (kJ/mol, $x \equiv x_{In}$):

$$G_{(\beta-Gd)} = (1-x)G^T_{Gd} + xG^T_{In} + RT(x\ln x + (1-x)\ln(1-x)) + (-110.7 + 0.0252T)x + 47x^2;$$

$$G_{Gd_2In} = (1-x)G^T_{Gd} + xG^T_{In} - 38.7 + 0.0084T + (-113.8 + 0.0267T)(x - 1/3) + 10000(x - 1/3)^2;$$

$$G_{Gd_{10}In_9} = (1-x)G^T_{Gd} + xG^T_{In} - 48 + 0.011T + (-30.6 + 0.0128T)(x - 9/19) + 2000(x - 9/19)^2;$$

$$G_{Gd_3In_5} = (1-x)G^T_{Gd} + xG^T_{In} - 50.3 + 0.0132T + (9.5 + 0.0059T)(x - 5/8) + 3000(x - 5/8)^2.$$

While accordingly to [8, 17], α-Gd also gives a wide range of solid solutions of In, we did not considered this, because: 1—that range has no equilibrium with the Gd–In melt, the thermodynamic properties of which are the principal studying object of the present work; 2—there are no exact data on the concentration bounds of those solid solutions. Due to similar reasons, the homogeneity ranges of all intermetallics are also tentative. The enthalpies and entropies of formation of all associates and intermetallics were considered independent on temperature.

We also calculated the activities of the components of melts of the Gd–In system (Fig. 2). It is obvious that they show great negative deviations from the Raoult's law. Similarly to the enthalpies of mixing of the melts, the activities are characterized by almost symmetrical outlook, with a weak shift of the ΔH and ΔG minima to the indium side. Accordingly to IAS model, the simplest associate GdIn reaches the greatest concentrations in the melts.

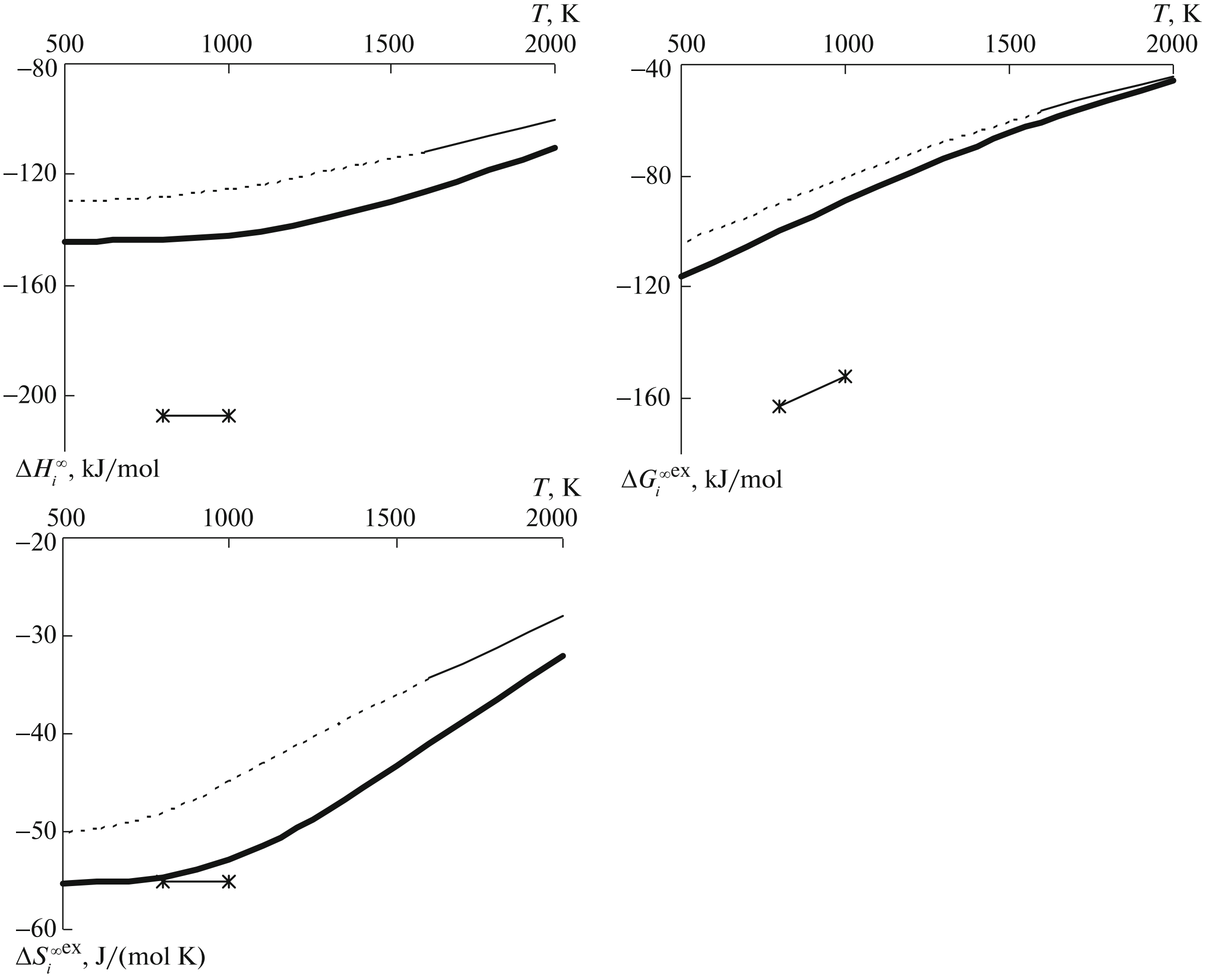

Fig. 3. The dependence of the partial enthalpies, excess Gibbs energies and entropies of components of the Gd–In melts at infinite dilution on temperature (━━━ Gd in In, ——— In in Gd, - - - - - - - In in undercooled Gd), accordingly to IAS model, and data from the literature [16] (✳——✳ Gd in In).

The temperature dependences of the partial enthalpies, Gibbs energies and entropies of the components of the Gd–In melts at infinite dilution (Fig. 3) are characterized by slow tendency to ideal solution at higher temperatures, which is in agreement with the general regularities [26]. A slow change of ΔH vs. temperature at 1600 K and the range close to it is a justification for neglecting the differences between the temperatures of our various experiments and 1600 K, made to simplify the calculations. Modeled values of $\Delta\overline{S}_{\mathrm{Gd}}^{\infty ex}$ agree with the data [16], but the absolute values of $\Delta\overline{H}_{\mathrm{Gd}}^{\infty}$ and $\Delta\overline{G}_{\mathrm{Gd}}^{\infty ex}$ are significantly smaller comparing to the literature. This may be explained by high inaccuracy of determining $\Delta\overline{H}_{\mathrm{Gd}}^{\infty}$ in [16] by indirect e.m.f. method.

The enthalpies and Gibbs energies of formation of the $\mathrm{GdIn_3}$ intermetallic, optimized by us (Figs. 4, 5), agree with less exothermic among the data from literature [10–15], as well as with the Miedema model [27]. The model [27] gives $\Delta\overline{H}_{\mathrm{Gd}}^{\infty} = -148$ kJ/mol, $\Delta\overline{H}_{\mathrm{In}}^{\infty} = -140$ kJ/mol for the liquid alloys. This agrees qualitatively with our experimental results ($\Delta\overline{H}_{\mathrm{Gd}}^{\infty} = -126.5 \pm 6.7$ kJ/mol; $\Delta\overline{H}_{\mathrm{In}}^{\infty} = -111.6 \pm 7.0$ kJ/mol), and correctly reflects almost symmetrical shape of the concentration dependence of ΔH, with a little shift of the minimum towards In (the component with smaller atomic volume).

The calculated liquidus and solidus curves of the phase diagram (Fig. 6) agree well with the literature data [7, 8, 17], excluding the range $0.34 < x_{\mathrm{In}} < 0.37$, where our model cannot confirm the possibility of a deep eutectic between the compounds $\mathrm{Gd_2In}$ and $\mathrm{Gd_5In_3}$.

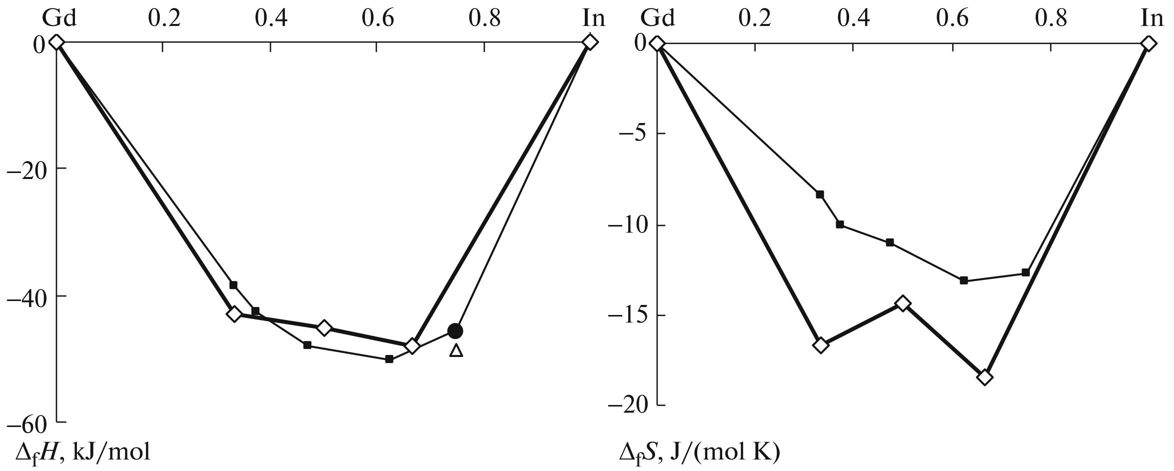

Fig. 4. Enthalpies and entropies of formation of the associates in the melt (—◇—) and intermetallics (—■—) of the Gd–In system, accordingly to our optimized thermodynamic model, and $\Delta_f H^{298}_{\mathrm{GdIn}_3}$ from literature: ● [14], △ [15].

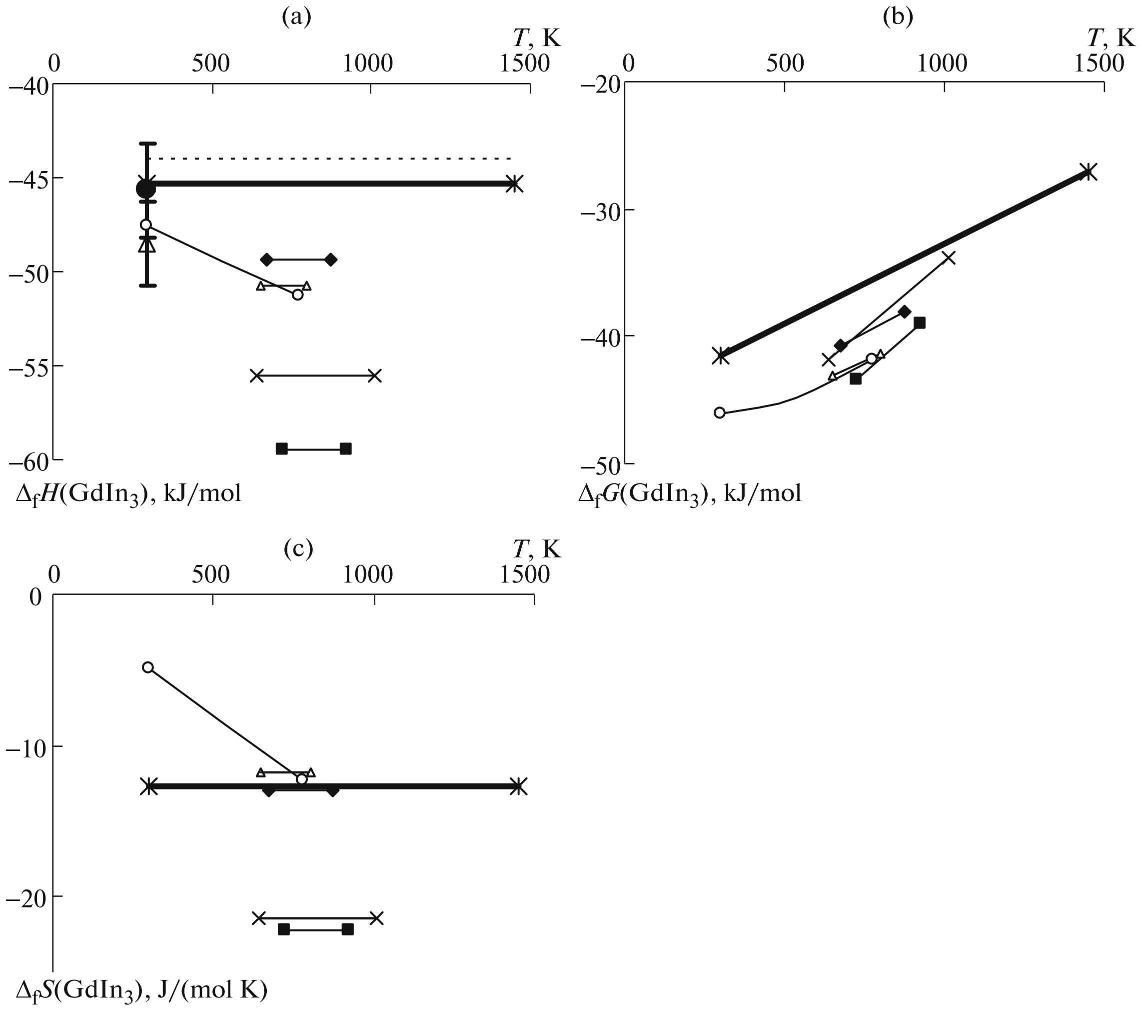

Fig. 5. Enthalpies (a), Gibbs energies (b), and entropies (c) of formation of the GdIn_3 intermetallic compound from pure solid components, determined in literature using e.m.f. method (—■— [10], —◆— [11], —△— [12], —×— [13]), calorimetry (● [14], △ [15]), estimated from the dependence on the atomic number of Ln for the Ln–In systems (—○— [19]), by Miedema model (---- [27]), and optimized by us in the present work (—✳—).

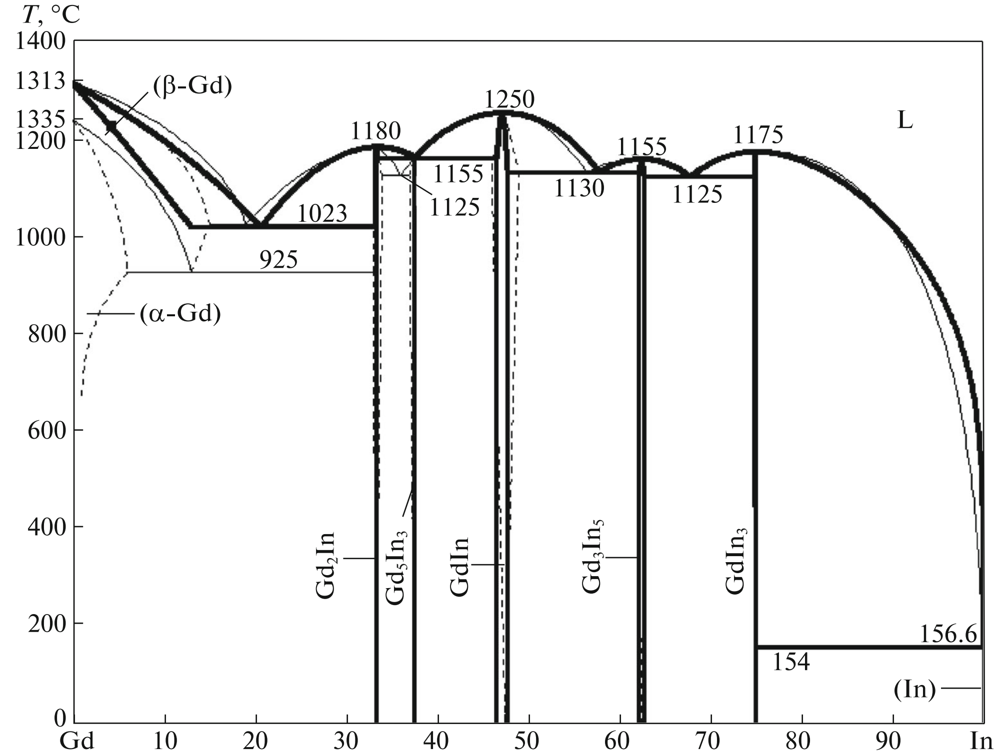

Fig. 6. Modeled phase diagram of the Gd–In system (bold liquidus and solidus curves), compared to the data from literature [17].

Therefore, the experimentally investigated enthalpies of mixing of melts of the Gd–In system are great exothermic values over the whole range of concentrations. The activities of the components, the Gibbs energies and the entropies of mixing of melts of this system, as well as its phase diagram, agree with most data in literature. Basing on our new results and the data from literature, an optimized thermodynamic model of the Gd–In system for the wide range of concentration and temperature is obtained for the first time.

REFERENCES

1. S. P. Yatsenko, *Indium. Properties and Application* (Nauka, Moscow, 1987) [in Russian].
2. Y. Wei, X. Su, F. Yin, Z. Li, X. Wu, and C. Chen, J. Alloys Compd. **333**, 118 (2002).
3. F. Gao, S. L. Wang, C. P. Wang, and X. J. Liu, CALPHAD: Comput. Coupling Phase Diagrams Thermochem. **35**, 1 (2011).
4. V. V. Berezutskii, M. I. Ivanov, M. A. Shevchenko, and V. S. Sudavtsova, Powder Metall. Met. Ceram. **53**, 693 (2015).
5. Y. Zhuang, S. Yuan, and J. Zheng, Acta Phys. Sin. (China) **31**, 121 (1982).
6. A. A. Semyannikov and S. P. Yatsenko, in *Synthesis and Properties of Rare Earth Element Compounds*, Ed. by V. G. Bomburov (Akad. Nauk SSSR, Ural. Nauch. Tsentr, Sverdlovsk, 1982), p. 123 [in Russian].
7. S. Delfino, A. Saccone, and R. Ferro, Z. Metallkd. **74**, 674 (1983).
8. A. Palenzona and S. Cirafici, Bull. Alloy Phase Diagrams **10**, 234 (1989).
9. E. N. Dieva, Tr. Inst. Khim., Ural. Nauch. Tsentr AN SSSR **29**, 98 (1974).
10. S. P. Vdovkina, V. A. Degtyar, L. A. Vnuchkova, and V. V. Serebrennikov, Tr. Tomsk. Univ., No. 249, 143 (1973).
11. A. P. Bayanov, Yu. A. Afanas'ev, and N. M. Pogorel'skaya, Zh. Fiz. Khim. **47**, 2105 (1973).
12. Din Khue Wu, V. P. Vasil'ev, and V. P. Gerasimov, in *Proceedings of the All-Union Conference on Calorimetry and Chemical Thermodynamics, Ivanovo, Sept. 25–27, 1979.*
13. V. I. Kober, I. F. Nichkov, S. P. Raspopin, and V. M. Kuz'minykh, *The Rare Metals Alloys with Special Properties: Rare-Earth and Precious Metals,* Ed. by E. M. Savitskii (Nauka, Moscow, 1983), p. 132 [in Russian].
14. A. Palenzona and C. Cirafici, Thermochim. Acta **9**, 419 (1974).
15. S. V. Meschel and O. J. Kleppa, J. Alloys Compd. **337**, 115 (2002).
16. V. A. Lebedev, *Thermochemistry of Alloys of Rare Earth and Actinide Elements, Reference Book,* Ed. by V. A. Lebedev, V. I. Kober, and L. F. Yamshchikov (Metallurgiya, Chelyabinsk, 1989) [in Russian].
17. *Binary Alloy Phase Diagrams,* Ed. by T. B. Massalski, 2nd ed. (ASM International, Metals Park, OH, 1990).

18. B. Predel, in *Landolt–Börnstein, New Series,* Vol. IV/5 (1996).
19. V. P. Vassiliev, A. Benaissa, and A. F. Taldrik, J. Alloys Compd. **572**, 118 (2013).
20. M. Ivanov, V. Berezutski, and N. Usenko, J. Mater. Res. **102**, 277 (2011).
21. A. T. Dinsdale, CALPHAD: Comput. Coupling Phase Diagrams Thermochem. **15**, 319 (1991).
22. V. G. Kudin, M. A. Shevchenko, I. V. Mateiko, and V. S. Sudavtsova, Zh. Fiz. Khim. **87**, 364 (2013).
23. M. A. Shevchenko, M. I. Ivanov, and V. V. Berezutskii, V. G. Kudin, and V. S. Sudavtsova, Russ. J. Phys. Chem. A **88**, 897 (2014).
24. V. S. Sudavtsova, M. A. Shevchenko, V. V. Berezutskii, M. I. Ivanov, and V. G. Kudin, Russ. J. Phys. Chem. A **88**, 200 (2014).
25. M. A. Shevchenko, V. G. Kudin, and V. S. Sudavtsova, in *Modern Problems of Physical Materials Science,* Tr. Inst. Prikl. Mat. (IPM im. Frantsevicha NANU, Kiev, 2012), Vol. 21, p. 67 [in Russian].
26. G. Kaptay, Metall. Mater. Trans. A **43**, 531 (2012).
27. F. R. de Boer, R. Boom, W. C. M. Mattens, A. R. Miedema, and A. K. Niessen, in *Cohesion and Structure,* Ed. by F. R. de Boer and D. G. Pettifor (North–Holland, Amsterdam, 1988).